Theoretical Model of a Thulium-doped Fiber Amplifier Pumped at 1570 nm and 793 nm in the Presence of Cross Relaxation

M A Khamis and K Ennser

***Abstract*— The static behavior of a Thulium doped fiber amplifier (TDFA) operating around 2 μm region at different pump wavelengths is investigated in this paper. A theoretical model is built up by solving a set of rate and propagation equations with considering the effect of cross relaxation mechanism. The developed model provides the influences of the amplified spontaneous emission (ASE) noise, seed wavelength and the thulium-doped fiber length into the TDFA performance. Simulation results indicate that the TDFA performance with pump at 1570 nm is more efficient than pump at 793 nm for core pumped thulium-doped silica fiber. Our findings show that the maximum gain reaches up to 30 dB with a 27 dBm pump power when a -10 dBm seed wavelength at 1840 nm is used. In contrast to indirect pumping at 793 nm, only 22 dB maximum gain is achieved under the same conditions. The model is also validated with previous experimental work. Our simulations are consistent with the experimental findings with small variations.**

***Index Terms*—Thulium-doped fiber amplifier, amplified spontaneous emission, silica glass material, cross relaxation process.**

I. Introduction

OVER the past few years, fiber laser sources around 2 μm are emerging as an attractive technology for a large number of researches. There are many applications for instance longer-wavelength laser pumping, atmospheric measurements, laser radar, laser plastics material processing, gas detection, biomedical and medical applications such as laser angioplasty, ophthalmic procedures, laser lithotripsy, and laser surgeries [1-5]. More recently the wavelengths around 2 μm have been proposed as a potential new window of data transmission for several reasons. Firstly, the hollow-core photonic band gap offers low loss window at 2 μm [6,7]. Secondly, thulium-doped fiber amplifiers (TDFAs) have recently been developed and characterized for optical communications, indicating low noise amplification and high gain in the 2 μm spectral region [8]. Finally, the emission spectrum of the $^3H_4$ – $^3H_6$ transition in TDFA covers about 30 THz (1700-2100 nm) of amplification bandwidth in a single device more than two times that of the erbium-doped fiber amplifier (EDFA) with the same configuration and complexity [9].

Two kinds of pumping approaches have already been proposed for TDFAs and lasers at 2μm: fiber laser pumping at 1558 nm (in-band pumping) [10] and diode pumping at 795 nm (indirect pumping) [11]. In-band pumping has limited diffraction and a significantly brighter beam than indirect pumping; these are important attributes for power scaling [12]. In contrast, it has been determined that high efficiency lasers can be reached by an indirect pumping due to the so-called cross-relaxation process [13]. The Tm^{3+} cross-relaxation is a non-radiative process in which two thulium ions in the $^3H_4$ upper laser level can be generated by a single excited thulium ion in the $^3F_4$ level [14]. Experiments using thulium-doped fibers indicate that the probability of the Tm^{3+} cross-relaxation strongly depends on the doping concentration. In addition, it is necessary to consider the influences of cross relaxation even at in-band pumping which lead to reduced the laser efficiency [15]. However, high Tm^{3+} doping concentration is restricted in silica glass therefore the cross relaxation process is limited in the fiber lasers. Furthermore, silica glass is not an ideal host for the 2 μm laser transition because of the high phonon energy (1100 cm^{-1}) of the silica glass network. As it can significantly quench the upper laser level and dramatically lower the quantum efficiency. Consequently, the output power and the quantum efficiency of Tm^{3+} silica fiber lasers are quite limited [16]. Thus, we select the Thulium concentration at 1.25 wt% and co-doped fiber with alumina to avoid the concentration quenching.

To achieve the best performance of practical systems, it is necessary to optimize the characteristics of lasers and amplifiers by using theoretical modeling and simulation. There are a lot of theoretical modeling results published for erbium and ytterbium-doped fiber lasers and amplifiers [17,18]. However, there are only a few works on the theoretical modeling and simulation of thulium-doped fiber lasers and amplifiers at 2 μm [19,20]. In addition these models do not take into account the influence of the amplified spontaneous emission noise on the performance of the lasers or amplifiers. Furthermore, there is no fair comparison of the TDFA performance for the different pump wavelength schemes at $^3H_4$ – $^3H_6$ transition. Jackson et al. [21] have demonstrated that an in-band laser outperforms indirect

Submitted on July 26, 2016. This work was supported in part by the European Community MPNS COST Action MP1401 "Advanced fiber laser and coherent source as tools for society, manufacturing and life science."

M. A. Khamis and K. Ennser are with College of Engineering, Swansea University, Swansea, Wales, UK (email: k.ennser@swansea.ac.uk).

pumping, but they determined this without considering ASE noise or the cross relaxation effect on in-band pumping scheme. In addition, the results of that study are focused on the characteristics of a laser, not an optical amplifier.

Here, we present a theoretical model of thulium-doped fiber amplifiers operating at 2 μm by solving a set of rate and propagation equations for in-band and indirect pumping, and taking into account the influences of cross relaxation in both pump schemes. Our model considers the effect of amplified spontaneous emission noise, the wavelength of the seed, as well as the length of the thulium-doped fiber. A MATLAB program is developed to investigate the TDFA performance when the thulium-doped silica fiber is pumped into the $^3H_4$ (in-band pumping) and into the $^3F_4$ (indirect pumping) absorption bands. Finally, the simulation results are compared with the published experimental measurements to check and evaluate the accuracy of our model.

II. Numerical Modeling of TDFA

The lowest Thulium-energy levels are sketched in Fig.1 where the pump, signal transition and the cross relaxation C mechanisms are indicated. According to the chosen pumping scheme, a separate numerical model is constructed based on Jackson [21] and added the influence of cross relaxation mechanism at both pump schemes. The numerical model consists on the rate equation of the electronic excitation in the thulium ions. The atomic rate equations describe the interaction between the pump, the signal and the ASE light in the TDFA. The populations in the energy levels can be estimated from the rate equations under any pump and signal power conditions. Figure 1 shows the four lowest energy manifolds of trivalent thulium ions. The population density N_2 is ignored [24] because the lifetime of this energy level is quite short typically 0.007 μs compared with other energy levels. Hence, most of the thulium ions at level 2 are rapidly transferred to energy level 1 by nonradiative relaxation.

The pump transition W_{p03}, W_{p01} and W_{p10}, signal transition W_{s01} and W_{s10}, and cross relaxation process C are indicated. The energy manifolds are numbered 0–3, and these denominations will be used throughout our model. Notes the model assumes that only the core of the fiber is pumped.

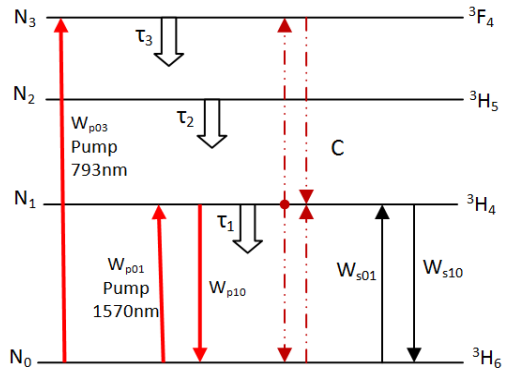

Fig. 1. Simplified energy level diagram of Tm^{3+} ions displaying. The pump and laser transitions are indicated as solid arrows together with the energy transfer mechanisms. The dash lines represent the cross relaxation process C.

A. Model for in-band pumping scheme

Based on Jackson's model and incorporating the cross relaxation process [15], the rate equations modeling of the thulium-doped fiber amplifier at any position along the thulium-doped fiber length at the in-band pump scheme when the $^3H_4$ energy level is directly excited are as follows:

$$\frac{dN_3(z,t)}{dt} = -\frac{N_3(z,t)}{\tau_3} - C \tag{1}$$

$$\frac{dN_1(z,t)}{dt} = w_{p01} - w_{p10} - \frac{N_1(z,t)}{\tau_1} + \frac{\beta_{31}N_3(z,t)}{\tau_3} - w_{s10} + w_{s01} + 2C \tag{2}$$

$$N_0(z,t) = N_T - N_1(z,t) - N_3(z,t) \tag{3}$$

Where C is the cross relaxation process and is given by:

$$C = k_{3101}N_0(z,t)N_3(z,t) - k_{1310}N_1^2(z,t) \tag{4}$$

Here τ_1 and τ_3 are the spontaneous lifetime of $^3H_4$ and $^3F_4$ levels, $N_0(z,t)$, $N_1(z,t)$, $N_3(z,t)$ are the population densities of $^3H_6$, $^3H_4$ and $^3F_4$ levels respectively, N_T is the Tm^{3+} concentration and set to be a constant; β_{31} is the branching ratio of the spontaneous transition from level 3 to 1. k_{3101} and k_{1310} are the cross-relaxation constants. w_{p01} is the pumping rate from $^3H_6$ to $^3H_4$ and w_{p10} represents the de-excitation of the $^3H_4$ level, w_{s10} is the stimulated emission rate from $^3H_4$ to $^3H_6$, and w_{s01} is the stimulated absorption rate from $^3H_6$ to $^3H_4$. The expressions of w_{p01}, w_{p10}, w_{s10} and w_{s01} are given as follow:

$$w_{p01} = \frac{\lambda_p\Gamma_p}{hcA_{core}}\sigma_a(\lambda_p)N_0(z,t)\left[p_p^-(z) + p_p^+(z)\right]. \tag{5}$$

$$w_{p10} = \frac{\lambda_p\Gamma_p}{hcA_{core}}\sigma_e(\lambda_p)N_1(z,t)\left[p_p^-(z) + p_p^+(z)\right]. \tag{6}$$

$$w_{s01} = \frac{\lambda_s\Gamma_s}{hcA_{core}}\sigma_a(\lambda_s)N_0(z,t) \times[p_s(z) + ASE_f(z) + ASE_b(z)]. \tag{7}$$

$$w_{s10} = \frac{\lambda_s\Gamma_s}{hcA_{core}}\sigma_e(\lambda_s)N_1(z,t) \times[p_s(z) + ASE_f(z) + ASE_b(z)]. \tag{8}$$

Where h is the Planck constant; c is the light speed in vacuum; λ_p and λ_s are the wavelengths of the pump light and the signal light in vacuum, respectively; Γ_p and Γ_s are the confinement factor for the pump and the signal, respectively; A_{core} is the cross-section area of the fiber core; $\sigma_a(\lambda_p)$ and $\sigma_a(\lambda_s)$ are the absorption cross sections of the pump light and the signal light, respectively; $\sigma_e(\lambda_p)$ and $\sigma_e(\lambda_s)$ are the emission cross-sections of the pump light and the signal light, respectively; $P_p^{\pm}(z)$ and $P_s(z)$ are the pump (corresponding to forward and backward) and the signal power at position z;

$ASE_f(z)$ and $ASE_b(z)$ are the forward and backward amplified spontaneous emission power at position *z*. Meanwhile, the power distributions of the pump light and the signal light along the fiber length can be expressed by the following propagation equations:

$$\frac{dp_p^{\pm}}{dz} = \pm p_p^{\pm}(z)[\ \Gamma_p(\sigma_e(\lambda_p)N_1(z) - \sigma_a(\lambda_p)N_0(z))\text{-}\alpha_p] \quad (9)$$

$$\frac{dp_s}{dz} = p_s(z)[\ \Gamma_s(\sigma_e(\lambda_s)N_1(z) - \sigma_a(\lambda_s)N_0(z))\text{-}\alpha_s] \quad (10)$$

The positive sign in (9) relates to the forward direction and negative sign to the reverse direction. The distribution of the ASE power along the fiber length can be established as follows [22,23]:

$$\frac{dASE_f}{dz} = ASE_f(z)[\ \Gamma_s(\sigma_e(\lambda_s)N_1(z) - \sigma_a(\lambda_s)N_0(z))\text{-}\alpha_s] + 2\sigma_e(\lambda_s)N_1(z)\frac{hc^2}{\lambda_s^3}\Delta\lambda \quad (11)$$

$$\frac{dASE_b}{dz} = -ASE_b(z)[\ \Gamma_s(\sigma_e(\lambda_s)N_1(z) - \sigma_a(\lambda_s)N_0(z))\text{-}\alpha_s] - 2\sigma_e(\lambda_s)N_1(z)\frac{hc^2}{\lambda_s^3}\Delta\lambda \quad (12)$$

Where α_p and α_s are the intrinsic absorption at the pump and signal wavelength for the Thulium-doped fiber, respectively, $\Delta\lambda$ is the bandwidth of the amplified spontaneous emission (ASE) around 2 μm.

B. Model for indirect pumping scheme

When the $^3F_4$ thulium energy level is pumped directly, the system of rate equations includes the cross-relaxation mechanism. The general rate equations for the thulium energy levels at any point along the length of the fiber are given by eq. (13-15). Based on Jackson [21] and under different approximation conditions include neglected the population inversion of $^3H_5$ energy level and the influences of the power up conversion process [24,25].

$$\frac{dN_3(z,t)}{dt} = w_{p03} - \frac{N_3(z,t)}{\tau_3} - \mathrm{C} \quad (13)$$

$$\frac{dN_1(z,t)}{dt} = \text{-}w_{s10} + w_{s01} - \frac{N_1(z,t)}{\tau_1} + \frac{\beta_{31}N_3(z,t)}{\tau_3} + 2C \quad (14)$$

$$N_0(z,t) = N_T - N_1(z,t) - N_3(z,t) \quad (15)$$

The term expressions of w_{s01}, w_{s10}, ASE_f and ASE_b can be taken from in-band pump model. Only the power distribution of the pump light along the fiber length is different. The de-excitation of the $^3H_4$ energy level in this pumping approach is omitted because there is no overlaps of the fluorescence emission spectrum with a portion of the pump absorption spectrum as in Fig.1 and therefore the pump distribution can be established as follows:

$$\frac{dp_p^{\pm}}{dz} = \mp p_p^{\pm}(z)[\ \Gamma_p(\sigma_a(\lambda_p)N_0(z)) + \alpha_p] \quad (16)$$

Note that the positive sign refers to the reverse direction and the negative to the forward direction.

III. RESULTS

At the steady condition, the time derivatives of eq. (1) to (3) for in-band pumping and (13) to (15) for indirect pumping are set to zero. All pump and signal power equations are first order differential equations, and the Runge-Kutta method is applied to solve the differential equations. Initially, the entire population is assumed to be at the ground level $^3H_6$ in the numerical calculations. The ode45 and fsolve Matlab functions are applied to solve the first order differential equations and the nonlinear equations, respectively. We use thulium-doped fiber (TmDF200) as an active fiber in these simulation and spectroscopy parameters of this fiber are summarized in table I [26]. Note that the cross relaxation parameters, the value of intrinsic absorption at the signal wavelengths and pump wavelength 793 nm are taken from [27]. We also calculate the absorption cross section of pump at 793 nm from the following eq. [28]:

$$\sigma_p = \frac{\alpha_p}{4.343\Gamma_p N_T} \quad (17)$$

TABLE I
VALUES OF NUMERICAL PARAMETERS

Symbol	Quantity	Value
N_T	Thulium concentration.	8.4×10^{25} m^{-3}
τ_1	Lifetime of level $^3H_4$.	650 μs
τ_3	Lifetime of level $^3F_4$.	12 μs
λ_{p1}	In-band pump wavelength.	1570 nm
λ_{p2}	In direct pump wavelength.	793 nm
λ_s	Signal wavelength.	1840 nm
σ_a(*793nm)*	Laser absorption cross section at 793nm.	7.8×10^{-25} m^2
σ_a(*1570nm)*	Laser absorption cross section at 1570nm.	2×10^{-25} m^2
σ_a(1840nm)	Laser absorption cross section at signal wavelength1840nm.	0.65×10^{-25} m^2
σ_e(1840)	Laser emission cross section at signal wavelength 1840nm.	3.7×10^{-25} m^2
A	Cross sectional area of the core.	3.01×10^{-11} m^2
α_p(793nm)	Intrinsic absorption at the pump wavelength 793 nm.	1.2×10^{-2} m^{-1}
α_p(1570nm)	Intrinsic absorption at the pump wavelength 1570 nm.	1×10^{-2} m^{-1}
α_s	Intrinsic absorption at the signal wavelength.	2.3×10^{-3} m^{-1}
K_{0131}	Cross relaxation constant.	3×10^{-23} m^3s^{-1}
K_{1310}	Inverse cross relaxation constant.	2.4×10^{-24} m^3s^{-1}

The initial conditions for the pump power, the signal power and the ASE spectrum in forward and backward directions are shown in table II [29]. The relaxation method is applied to solve the boundary conditions and to achieve the accuracy of less than 0.01% for the pump, the signal and the ASE powers [29]. The thulium-doped fiber of length L is divided into N segments along the z-direction. The equations are solving for the pump, the signal and the ASE power propagating in the first segment (segment 0) by using the above initial conditions without considering ASE_b. For the following segments (segment 1 to N-1), the power for the pump, the signal and the ASE at one end of a segment is applied as the input for the next segment. Then the whole set of equation are integrated back from $z = L$ to $z = 0$ with initial value ASE_b =0 to obtain the pump, the signal, ASE_f and ASE_b power propagating for the whole segments as previously illustrated. To improve our modeling accuracy, the system is then integrated back and forth (from z= 0 to $z = L$, and then from $z = L$ to $z = 0$). In our simulation, the iteration of this integration routine will be stopped after achieving less than 10^{-7} of the successive solutions difference. Using the data of Table I and the values of the emission and the absorption cross-section spectra [26], we solve numerically the rate equations of the two pump models.

TABLE II
INITIAL CONDITIONS

Initial condition	Explanation
$P_p^+(z=0)$ = Forward launched pump power.	Initial condition for 1570nm and 793nm pumps at z=0.
$P_p^-(z=L)$ =Backward launched pump power.	Initial condition for 1570nm and 793nm pumps at z=L.
P_s (z=0)= seed power.	Initial condition for seed power at z=0.
ASE_f (z=0)=0	Initial condition for forward amplified spontaneous emission at z=0.
ASE_b (z=L)=0	Initial condition for backward amplified spontaneous emission at z=L.

Initially, we evaluate the optimum thulium-doped fiber length for each of the two pumping schemes. The forward launched pump configuration will be used in these simulations with 27 dBm (0.5 W) total pump power. Figure 2 and 3 illustrate the theoretical prediction of the output power and the residual pump power at in-band and indirect pumping scheme, respectively when the fiber core is seeded by a -10 dBm signal at 1840 nm. As shown in Fig. 2, the distribution of the pump power reaches to zero at its optimum length of 1.25 m when pumped at 1570 nm and 0.5 m when indirect pumped (Fig. 3). The in-band pumped amplifier needs a longer length of thulium-doped fiber because the absorption-cross section at pump wavelength 1570 nm is lower than at 793 nm. As a result, the amplified spontaneous emission power and the gain are high when the pump wavelength is 1570 nm in comparison with the indirect pump case as illustrated in Figs. 4-7.

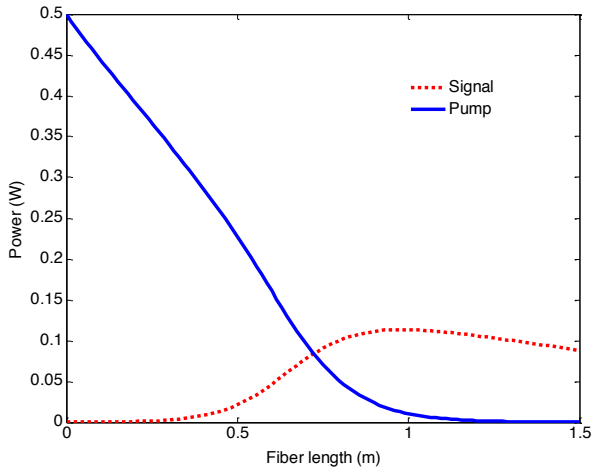

Fig. 2 The distribution of pump power (sold line) and signal power (dash line) at 1840 nm along the fiber length when the total launch pump power is 27 dBm and the seed power is -10 dBm at in-band pump.

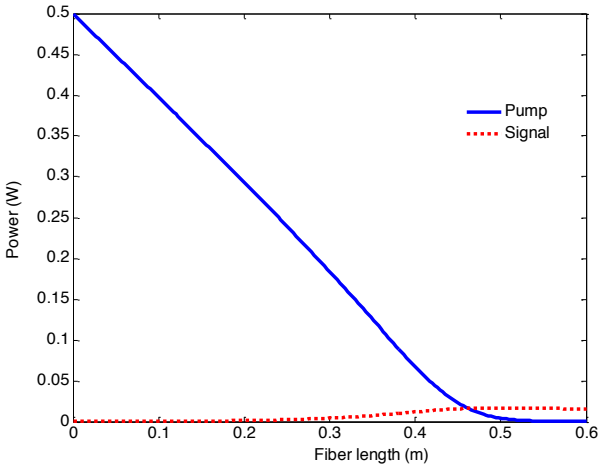

Fig. 3 The distribution of pump power (sold line) and signal power (dash line) at 1840 nm along the fiber length when the total launch pump power is 27 dBm and the seed power is -10 dBm at indirect pump.

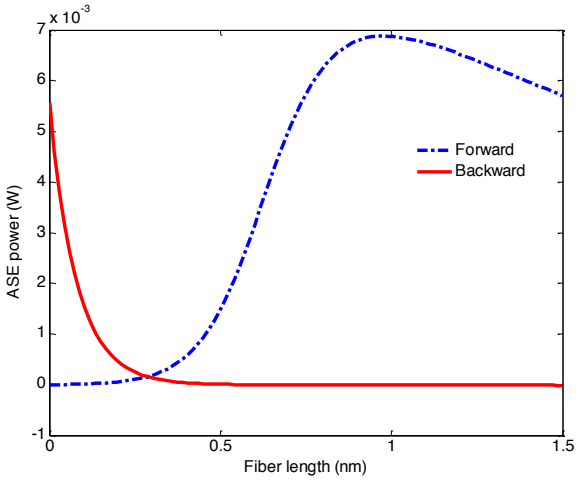

Fig. 4 The distribution of backward ASE power (sold line) and forward ASE power (dash line) at 1840 nm along the fiber length when the total launch pump power is 27 dBm and the seed power is -10 dBm at in-band pump.

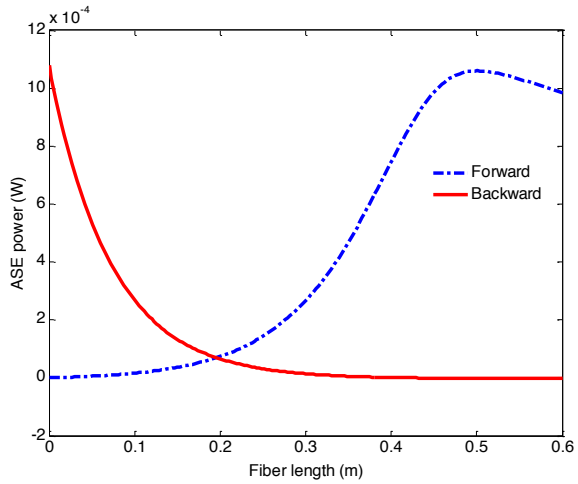

Fig. 5 The distribution of backward ASE power (sold line) and forward ASE power (dash line) at 1840 nm along the fiber length when the total launch pump power is 27 dBm and the seed power is -10 dBm at indirect pump.

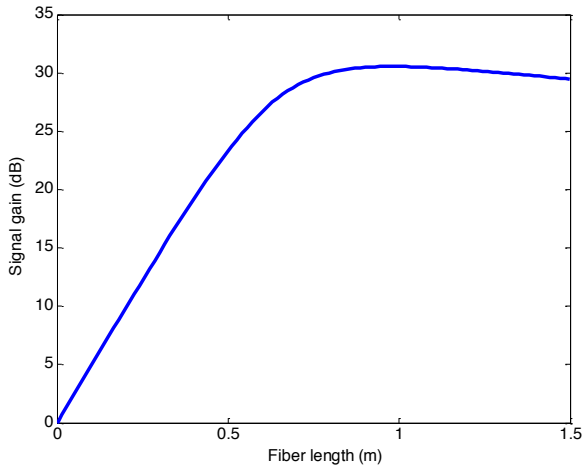

Fig. 6 The distribution of signal gain at 1840 nm along the fiber length when the total launch pump power is 27 dBm and the seed power is -10 dBm at in-band pump.

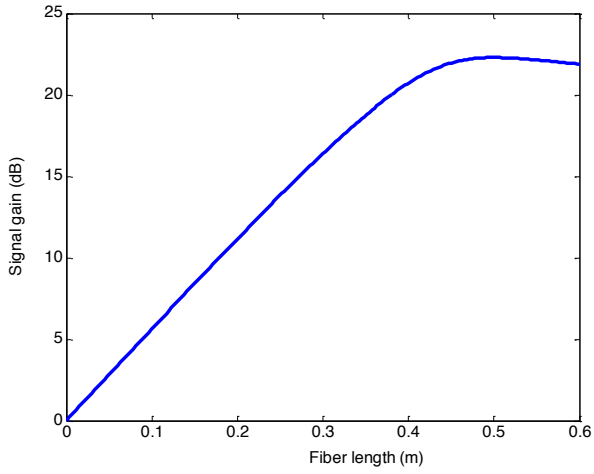

Fig. 7 The distribution of signal gain at 1840 nm along the fiber length when the total launch pump power is 27 dBm and the seed power is -10 dBm at indirect pump.

The last investigation in our study is to obtain the wavelength dependence of the small-signal gain and the noise figure when the signal wavelength varies from (1730-1950nm). For every wavelength we calculate the value of Γ_s and choose suitable values of $\sigma_e(\lambda_s)$ and $\sigma_a(\lambda_s)$ according to absorption and emission cross-section spectra [26] and applied it in our model to calculate the values of amplified output signal, ASE_f and ASE_b. After that we can calculate at every seed wavelength the signal gain (amplified output power/seed input power) and the noise figure by the equation [29]:

$$NF = \frac{1}{G} + \frac{P_{ASE}}{G\ h\ v\ \Delta v} \tag{18}$$

Where G and P_{ASE} is the gain and ASE power at the particular wavelength, respectively. Repeat this process for each seed wavelength and in every time we calculate the signal gain and noise figure. Figures 8 and 9 illustrate the small signal gain and noise figure versus seed wavelengths in-band pump and indirect pump scheme, respectively. Note that the pump and seed power is fixed at 27 dBm and -10 dBm, respectively for both cases of pump wavelengths. And also, 1.25 m and 0.5 m are the fiber lengths for in-band pump and indirect pump schemes, respectively. For in-band pumped amplifier the maximum gain signal reaches to 30 dB at 1840 nm with a full width at half-maximum (FWHM) bandwidth of 160 nm. Considerable lower gain and narrower bandwidth is obtained when using an indirect pumping scheme. As shown in Fig 9 only 22 dB maximum signal gain at 1840 nm is obtained with a FWHM bandwidth of 150 nm. The reason for the variation in the signal gain with respect to the seed wavelength is mainly because the emission cross-section reduces rapidly out of a certain range. Therefore the seed wavelength should be selected near the emission cross-section peak to produce high amplification. Thus it is important to give more attention in the selection of the seed wavelength. In addition, the value of the noise figure is around 6-6.5 dB between 1750-1950 nm at both pump schemes.

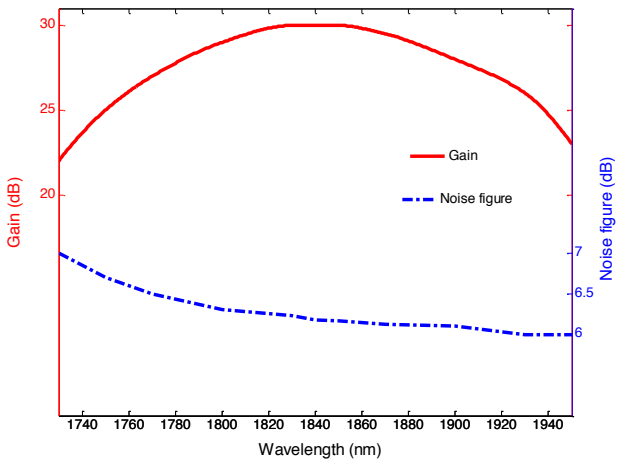

Fig. 8 Small signal gain and noise figure versus seed wavelength when the total launch pump power is 27 dBm and the seed power is -10 dBm at in-band pump.

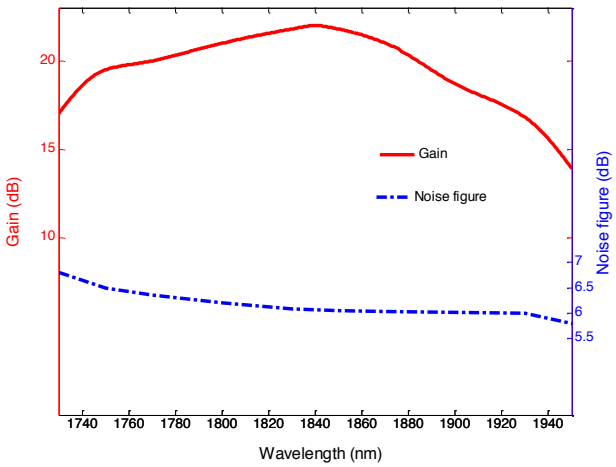

Fig. 9 Small signal gain and noise figure versus seed wavelength when the total launch pump power is 27 dBm and the seed power is -10 dBm at indirect pump.

IV. MODEL VALIDATION

To evaluate the accuracy and versatility of the model, it is necessary to compare our numerical results with the published experimental measurements. We use the model in a bidirectional configuration to demonstrate the wavelength dependence of the small-signal gain of TDFA at in-band pump with and without the cross relaxation influences CR, and to compare with the experimental results, which is reported in [30]. In fact when the active fiber has low thulium ion concentration the cross relaxation effect can be neglected [23,31]. In this paper we consider a commercial thulium doped fiber with sufficient thulium ion concentration to note the presence of the cross relaxation and it should be taking into account in the model. For a fair validation, we demonstrate a bidirectional configuration which is denoted as TDFA-A schematic in [30]. We choose the same pumped wavelength at 1570 nm and the spectroscopy parameters of thulium-doped fiber (TmDF200). In addition, we take the influence of the insertion loss of WDM coupler and isolator from the experimental work, which used a customer coupler with only 1 dB insertion loss of pump power. Also, according to the schematic of this coupler [30], the insertion loss of the seed power (1750nm-1950) is approximately 1 dB which loses 20.5% of the seed input power. We also take into account the wavelength dependence loss of the isolator from the schematic insertion loss [30] and apply it in both the seed input power and amplified output power. The total launched power for each direction equals to 24 dBm, the seed input power is -20 dBm and the thulium doped-fiber is 1m. The only assumption in our model is the intrinsic absorption at signal wavelengths and according to our numerical investigation it has a small impact on the results.

Figure 10 illustrates the small signal gain of our model with and without CR together with experimentally measured values. The maximum signal gain at 1840 nm is 36 dB when ignoring the cross relaxation in the modeling. In contrast, the maximum signal gain is 35 dB when taking into account the cross relaxation which is overlapping with the experimental work. Overall an excellent agreement is achieved between our modeling and the experimental findings with small variations due to possible splicing and connector losses.

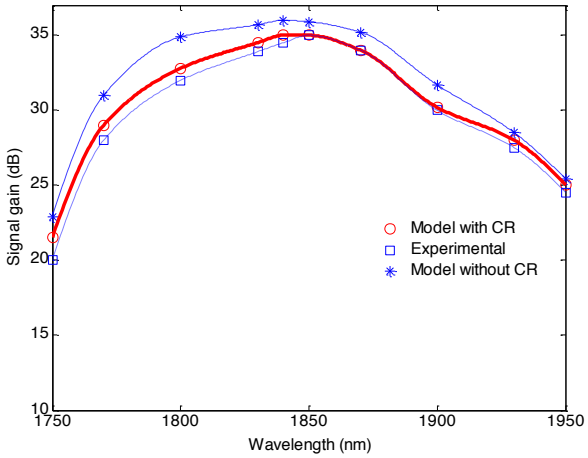

Fig. 10 Small signal gain dependence on the seed wavelength when the total launch pump power is 27 dBm and the seed power is -20 dBm at in-band pump in our model with and without CR and included experimental results.

V. CONCLUSIONS

We have presented a theoretical model of thulium-doped fiber amplifier around 2 μm for in-band and indirect pumping scheme. Based on a set of rate and propagation equations, a MATLAB program is developed with Runge-Kutta method to investigate the static behavior of the TDFA. The model provides the influences of the ASE noise, cross relaxation, fiber length and wavelength of the seed into the TDFA performance. This is the first time to our knowledge that a theoretical study of TDFA around 2 μm considering the influence of cross relaxation mechanism under different pump wavelengths has been thoroughly investigated.

The simulation results show that the signal gain at the in-band pump is higher than at the indirect pump with similar noise figure around 6 dB under the same conditions. In case of the in-band pump, the maximum gain reaches to 30 dB at 1840 nm seed wavelength with pump power of 27 dBm and signal power of -10 dBm. In the case of an indirect pump, the maximum gain is only 22 dB under the same conditions. As a result, TDFA pumped at in-band pump is more efficient with core pumped thulium-doped silica fiber. Finally, it is essential to pay more attention to the selection of the seed wavelength in the design of TDFA as high amplification gain can be achieved when the selection wavelengths are near the centre of emission cross-section curve. The model is validated with previous experimental work. Our simulations are consistent with the experimental findings with small variations only possibly due to splicing and connector losses, which gives confidence in the obtained results.

REFERENCES

[1] K. Thyagarajan and A. Ajoy 'Lasers: Fundamentals and Applications' Springer, 2010.

[2] S. W. Henderson, P. J. M. Suni, C. P. Hale, S. M. Hannon, J. R. Magee, D. L. Bruns, and E. H. Yuen, "Coherent laser radar at 2 μm using solid

state lasers," *IEEE Trans. Geosci. Remote Sens.*, vol. 31, no. 1, pp. 4–15, 1993.

[3] N. M. Fried, "Thulium fiber laser lithotripsy: An in vitro analysis of stone fragmentation using modulated 110-Watt thulium fiber laser at 1.94 μm," *Lasers Surg. Med.*, vol. 37, pp. 53–58, 2005.

[4] G. J. Koch, J. Y. Beyon, B. W. Barnes, M. Petro, J. Yu, F. Amzajerdian, M. J. Kavaya, and U. N. Singh, "High-energy 2 μm doppler lidar for wind measurements," *Opt. Eng.*, vol. 46, pp. 116201–116214, 2007.

[5] T. Bleuel, M. Brockhaus, J. Koeth, J. Hofmann, R. Werner and A. Forchel, "single-mode DFB lasers for gas sensing in the 2-µm wavelength range," Proc. SPIE 3858, Advanced Materials and Optical Systems for Chemical and Biological Detection, 1999.

[6] P. J. Roberts, F. Couny, H. Sabert, B. J. Mangan, D. P. Williams, L. Farr, M. W. Mason, A. Tomlinson, T. A. Birks, J. C. Knight, and P. St. J. Russell, "Ultimate low loss of hollow-core photonic crystal fibres," Opt. Express, vol. 13, no. 1, pp. 236-244, 2005.

[7] N. Mac Suibhne, Z. Li, B. Baeuerle and J. Zhao, "WDM Transmission at 2µm over Low-Loss Hollow Core Photonic Bandgap Fiber," in Optical Fiber Communication Conference/National Fiber Optic Engineers Conference 2013, OSA Technical Digest (online) (OSA, 2013), paper OW1I.6.

[8] Z. Li, S. U. Alam, J. M. O. Daniel, P. C. Shardlow, D. Jain, N. Simakov, A. M. Heidt, Y. Jung, J. K. Sahu, W. A. Clarkson and D. J. Richardson, "90 nm Gain Extension Towards 1.7 µm for Diode-Pumped Silica-Based Thulium-doped Fiber Amplifiers," in ECOC (2014). Paper Tu.3.4.2.

[9] Z. Liu, Z. Li and Y. Chen. "52.6Gbit/s Single-Channel Directly-Modulated Optical Transmitter for 2µm Spectral Region," Optical Fiber Communication Conference, OSA (2015), paper Th1E.6.

[10] T. Yamamoto, Y. Miyajima, and T. Komukai, "1.9µm Tm-doped silica fiber laser pumped at 1.57µm," Electron. Lett., vol. 30, pp. 220-221, 1994.

[11] P. F. Moulton, G. A. Rines, E. V. Slobodthikov, K. F. Wall and A. L. G. Carter, "Tm-doped fiber lasers: fundamentals and power scaling," IEEE J. Sel. Top. Quantum Electron., vol.15, pp. 85-91, 2009.

[12] D. Y. Shen, J. K. Sahu, and W. A. Clarkson, "High-power widely tunable Tm:fibre lasers pumped by an Er,Yb co-doped fiber laser at 1.6 µm," Opt. Express, vol.14, pp. 6084-6090, 2006.

[13] S. D. Jackson, "Cross relaxation and energy transfer upconversion process relevant to the functioning of 2µm Tm-doped silica fiber lasers," Opt. Commun., vol. 230, pp. 197-203, 2004.

[14] J. Geng, Q. Wang, T. Luo, S. Jiang and F. Amzajerdian, "Single-frequency narrow-line width Tm-doped fiber laser using silicate glass fiber," Opt. Lett., vol. 34, pp. 3493–3495, 2009.

[15] C. A. Evans, Z. Ikonic, B. Richards, P. Harrison and A. Jha, "Theoretical Modeling of a 2 µm Thulium Doped Tellurite Fiber laser: The Influence of Cross Relaxation," in *J. of Lightwave Technology*, vol. 27, no. 18, pp. 4026-4032, 2009.

[16] C. Daniel, R. Benjamin, R. Glen, and S. Scott, "High power resonant pumping of Tm-doped fiber amplifiers in core- and cladding-pumped configurations," Opt. Express, vol. 22, pp. 29067-29080, 2014.

[17] Y. Wang; H. Po, "Dynamic characteristics of double-clad fiber amplifiers for high-power pulse amplification," J. of Lightwave Technology, vol. 21, no.10, pp. 2262-2270, 2003.

[18] J. E. Crahay, P. Megret, P. Froidure, J.-C. Lamquin, M. Blondel, "Analysis of numerical methods efficiency for EDFA modeling," in *Electrotechnical Conference, 1994. Proceedings., 7th Mediterranean* , vol.1, pp. 12-14, Apr 1994.

[19] Y. L. Tang and J. Q. Xu, "Effects of excited-state absorption on self pulsing in Tm^{3+} doped fiber lasers," *J. Opt. Soc. Am. B*, vol. 27, no. 2, pp. 179–186, 2010.

[20] F. Wang, D. Shen, H. Chen, D. Fan, and Q. Lu, "Modeling and optimization of stable gain-switched Tm-doped fiber lasers," *Optical Review,* vol. 18, pp. 360-364, 2011.

[21] S. D. Jackson and T. A. King, "Theoretical modeling of Tm-doped silica fiber lasers," J. of Lightwave Technology, vol. 17, pp. 948-956, May 1999.

[22] Z. Y. Hu, P. Yan, Q. Liu, E. C. Ji, Q. R. Xiao, and M. L. Gong, "High-power single-stage thulium-doped superfluorescent fiber source," *Appl. Phys. B*, pp. 1–7, 2014.

[23] G. Yu, J. Chang, Q. Wang, X. Zhang, Z. Liu, and Q. Huang, "A theoretical model of thulium-doped silica fiber's ASE in the 1900 nm waveband," *Optoelectron. Lett.*, vol. 6, no. 1, pp. 45–47, 2010.

[24] Z.-Y. Hu, P. Yan, Q.-R. Xiao, Q. Liu, and M.-L. Gong, "227-W output all-fiberized Tm-doped fiber laser at 1908 nm," *Chinese Phys. B*, vol. 23, no. 10, p. 104206, 2014.

[25] J. Xu, M. Prabhu, J. Lu, K. Ueda, and D. Xing, "Efficient double-clad thulium-doped fiber laser with a ring cavity.," *Appl. Opt.*, vol. 40, no. 12, pp. 1983–1988, 2001.

[26] S. D Agger and J. H. Povlsen, "Emission and absorption cross section of thulium doped silica fibers," Opt. Exp.,vol. 14, no. 1, pp. 50–57, 2006.

[27] M. Tao, Q. Huang, T. Yu, P. Yang, W. Chen, and X. Ye, "Cross relaxation in Tm-doped fiber lasers," *Proc. SPIE 8796, 2nd Int. Symp. Laser Interact. with Matter (LIMIS 2012)*, no. September 2015, p. 87961W, 2013.

[28] M. M. Tao, P. L. Yang, Q. J. Huang, T. Yu, and X. S. Ye, "Parameters Determination and Theoretical Modeling of Tm-Doped Fiber Lasers," *Key Eng. Mater.*, vol. 552, no. May 2013, pp. 349–355, 2013.

[29] S. D. Emami, S. W. Harun, H. A. Rashid and H. Ahmad, " Thulium-Doped Fiber Amplifier, Numerical and Experimental Approach:, Nova Science Publishers, Inc., pp.15-60, 2011.

[30] Z. Li, Y. Jung, J. M. O. Daniel, N. Simakov, M. Tokurakawa, P. C. Shardlow, D. Jain, J. K. Sahu, A. M. Heidt, W. A. Clarkson, S. U. Alam, and D. J. Richardson, "Exploiting the short wavelength gain of silica-based thulium-doped fiber amplifiers," *Opt. Lett.*, vol. 41, no. 10, pp. 2197–2200, 2016.

[31] M.A. Khamis and K Ennser, "Model for a Thulium-doped Silica Fiber Amplifier Pumped at 1558nm and 793nm", International Journal of Engineering and Advanced Technology (IJEAT), vol. 5, no.4, 2016.